CHAPTER 6

Modern CFD application on aerothermal engineering aspects of natural draft cooling towers

D. Bohn[1] & K. Kusterer[2]
[1]*Institute of Steam and Gas Turbines, RWTH Aachen University, Aachen, Germany.*
[2]*B&B-AGEMA GmbH, Aachen, Germany.*

Abstract

Natural draft cooling towers are a very efficient way to provide the cold end of thermal power plants with a steam turbine cycle. The cooling tower shape, details of construction and arrangement and type of cooling fill have a significant influence on the cooling tower efficiency, in particular, on the cold water temperature that can be reached. Furthermore, influences of cross wind situations on the performance of the cooling tower are of high interest. Modern computational tools for three-dimensional flow simulations (CFD) can be coupled by local heat and mass transfer calculation schemes with the cooling water film calculation and thus allow a comprehensive numerical investigation of the aerodynamic and thermodynamic behaviour of natural draft cooling towers under specific operating conditions. After validating the numerical approach, the numerical method has been used for determination of the influences of fill types, of the inner rim structure at the tower outlet and of an additional flue gas discharge on the cooling tower performance. Furthermore, numerical calculations of several cross wind operating conditions have been performed. The numerical simulations show clearly that the equipment of the cooling tower with a modern fill-type achieve higher efficiencies. Cross wind situations lead to a significant reduction in the cooling tower efficiency and thus to higher cold water temperatures. A major result of the simulations is that under unfavourable circumstances, a periodic cold air ingestion at the tower outlet might appear that leads to unstable operating conditions with reduced efficiencies. The inner rim structure at the tower outlet has a stabilizing effect in cross wind situations.

WIT Transactions on State of the Art in Science and Engineering, Vol 42, © 2008 WIT Press
www.witpress.com, ISSN 1755-8336 (on-line)
doi:10.2495/978-1-84564-062-0/06

1 Introduction

Cooling towers provide the cold end for steam turbine cycles mainly used in thermal power plants for producing electricity. The objective of the cooling tower and condenser operation is to condense steam exiting from the low-pressure turbines at a pressure, which should be as low as possible to maximize the power output from the plant. The condenser pressure is thermodynamically linked to the cooling water temperature offered by the cooling tower. The closer it is to ambient temperature, the better it is for the cycle performance.

High efficiencies are typically achieved with wet cooling towers. In this design, cooling water heated in the condenser is cooled by convection and evaporation in contact with ambient air. The contact time and area between air and water are increased by spraying the water over a fill (a grid of bars or plates) and by passing air through the fill. The water to be cooled then trickles from the top through the cooling fills. The water is cooled in two ways when the cooling air is passing by. A small amount of water evaporates so that evaporative heat is extracted from the cooling water flow. Furthermore, heat is transferred from the water to the cooling air by convection.

Most efficient designs, although comparatively expensive, are based on buoyancy driven air flow. Natural draft cooling towers exist in two flow arrangements, a counterflow and a crossflow arrangement (see Fig. 1). In mechanical draft cooling towers, a fan provides the necessary air amount to the fill. Due to higher air velocities the heat transfer is enhanced and, thus, mechanical draft cooling towers are much smaller in size than natural draft cooling towers, but the necessary fan power reduces the overall power output of the plant. Modern natural draft cooling towers can be as high as 200 m or even more with base diameters of approximately 150 m. Figure 2 shows a typical natural draft cooling tower with a modern design including an additional flue gas discharge in the centre of the tower.

Natural draft cooling towers are very sensitive to special operation conditions, e.g. additional flue gas discharge and environmental conditions, e.g. cross wind effects. The incoming air in case of a cross wind situation is unevenly distributed to the fill and the buoyancy driven air flow in the tower might be affected by cold

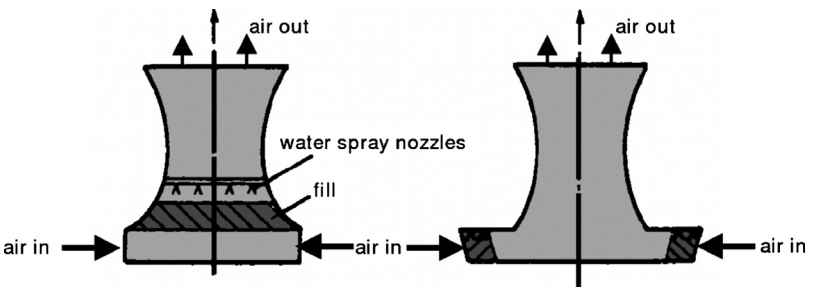

Figure 1: Natural draft cooling towers with counterflow (left) and crossflow (right) arrangement.

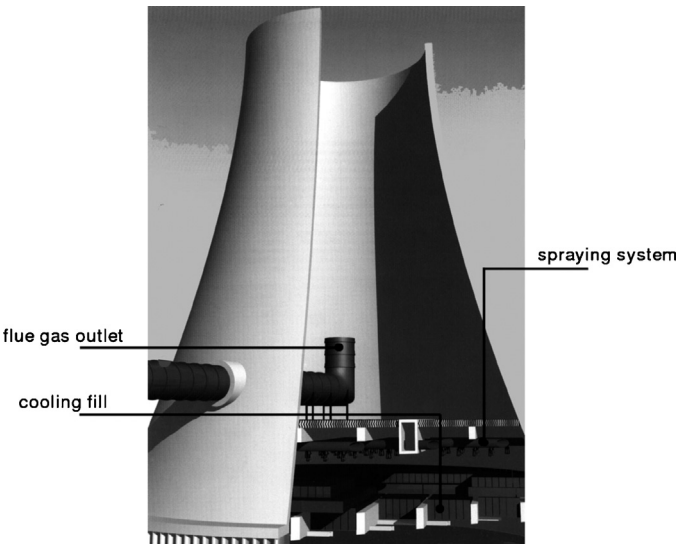

Figure 2: Modern natural draft cooling tower (counterflow arrangement).

air entering the tower from the top. The consequence of both influences is a distorted heat transfer distribution across the cooling tower cross section, leading to an overall reduction in the cooling tower efficiency. As a result, the cold water temperature increases and thus the efficiency and performance of the complete steam cycle are reduced.

Further improvements of natural draft cooling towers that lead to reduced cold water temperatures need not only a precise knowledge of the local heat transfer and flow conditions but also a detailed modelling of the interactions of heat- and mass transfer and the cooling tower aerodynamics with a comprehensive numerical approach. The numerical approach should combine the abilities of modern computational fluid dynamics (CFD) tools for calculation of three-dimensional steady and unsteady flow conditions in a cooling tower and the empirical heat and mass transfer correlations for special fill arrangements in the cooling tower as provided by the manufacturers.

Early collections of correlations and investigations on typical influences of parameters on the heat and mass transfer in cooling towers can be found in [1, 2]. With respect to the numerical calculation, an early approach that treats the air flow to be two-dimensional, while the water flow is considered to be one-dimensional, has been presented in the 1980s by Majumdar *et al.* [3, 4]. They have applied the numerical scheme to several examples for mechanical and natural draft cooling towers of both counterflow and crossflow designs. Major limitations in that time can be related to the lack of computational performance that did not allow using three-dimensional flow solvers and high-resolution numerical grids. Due to the significant progress in commercial software development

(computational fluid dynamics) and the great increase in computational abilities in the 1990s, today tools and computers are available for the comprehensive solution of all governing equations and their interactions, even for complex geometric models.

In this chapter, example results for a natural draft cooling tower application of commercial CFD tool [5] combined with specially developed subroutines on the heat and mass transfer for local coupling of the air-side and water-side calculations are presented. The results contain a validation of the aerodynamic and thermodynamic models and further present the effects of cooling tower design features and cross wind situations on the local flow behaviour and the overall cooling tower performance.

2 Numerical modelling

2.1 Implementation of a heat transfer and mass transfer model

The water-side and air-side flow in a wet cooling tower is a two-phase flow with complex heat transfer and mass transfer conditions between both fluids. Thus, the complete numerical simulation of all relevant conservation equations for the three-dimensional flow in cooling towers is still beyond the economical application for industrial use with respect to time and cost efforts. Therefore, a simplification is introduced by handling the wet air as a one-phase mixture of fluids consisting of the two components (1) dry air and (2) water steam. This is necessary to take into account the change in density due to the local wetness. In the following section, this one-phase model fluid is mentioned as "air" or "air-side."

The energy balance and mass balance between the cooling water film and the air can be established. Transferred heat and mass flow values are implemented as additional source terms to the governing equations for the calculations on the cooling film side and wet air flow. As the flow of the cooling water cannot be taken into account additionally to the air flow directly in the finite volume cells of the computational grid, information on inlet and outlet temperatures and the local mass flow for the cooling water flow have to be stored separately for every cell and have to be exchanged with the neighbouring cells in the flow direction of the water.

Figure 3 shows the important physical parameters of the mass and energy balance for the cooling water element and the air-side finite volume cell. For the energy balance of the cooling water element, the evaporative heat flux due to the evaporation process and the convective heat flux have to be taken into account. The local gradient of the temperature between the cooling water film and the air-side is determining the local convective heat flux, whereas the local gradient between the water content for the saturated moist air and the water content for the moist air is determining the local evaporation rate and, thus, the evaporative heat flux. For the convective heat flux calculation, the averaged temperature of the inlet and outlet temperature of the cooling water element is used. Furthermore, it is assumed that the local air condition directly in contact with the cooling water film is always

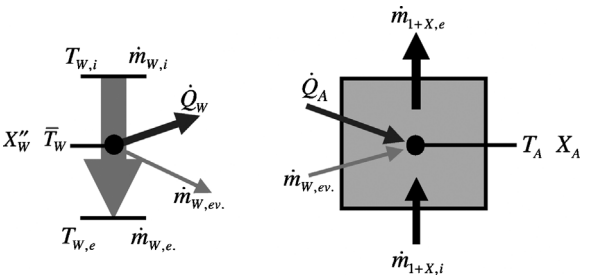

Figure 3: Physical parameters for heat and mass balances at a cooling water element (left) and a finite volume cell of the air-side (right).

saturated. Altogether, the local heat flux transferred from the cooling water element can be calculated as follows:

$$\dot{Q}_{\mathrm{W}} = \alpha \cdot A \cdot \left(\overline{T}_{\mathrm{W}} - T_{\mathrm{A}}\right) + \beta_x \cdot A \cdot \left(X''_{\mathrm{W}} - X_{\mathrm{A}}\right) \cdot \Delta h_{\mathrm{ev}} \tag{1}$$

In case the air in the finite volume cell is saturated with water as well as the air in contact to the cooling water film, but a temperature gradient between the cooling water film and the air-side is established, the diffusion process continues further despite the saturated air condition due to the gradient of the water content. This leads to a re-condensation of water on the air-side. The re-condensed water and small droplets taken away by mechanical forces are the reason for the visible plume at the cooling tower exit. The re-condensation of steam on the air-side is not part of the used numerical models up to now.

The outlet temperature of the cooling water for the cooling water element can be calculated based on the first law of thermodynamic as following:

$$T_{\mathrm{W,e}} = \frac{\left(\dot{m}_{\mathrm{w,i}} \cdot c_{\mathrm{W}} \cdot T_{\mathrm{W,i}} - \dot{Q}_{\mathrm{W}} - \dot{m}_{\mathrm{W,ev}} \cdot c_{\mathrm{W}} \cdot \overline{T}_{\mathrm{W}}\right)}{\dot{m}_{\mathrm{W,e}} \cdot c_{\mathrm{W}}} \tag{2}$$

The heat flux into the air-side finite volume cell is mainly determined by the convectively transferred heat:

$$\dot{Q}_{\mathrm{A}} = \alpha \cdot A \cdot \left(\overline{T}_{\mathrm{W}} - T_{\mathrm{A}}\right) + \dot{m}_{\mathrm{W,ev}} \cdot h''_{\mathrm{S}} \tag{3}$$

2.2 Evaporation number and Lewis analogy

The theoretical approach on the calculation of local mass transfer and heat transfer is mainly based on an evaporation number k_{V} (often also mentioned as Merkel number) for the determination of a mass transfer coefficient and the Lewis analogy for determination of a convective heat transfer coefficient.

The Merkel number is defined:

$$k_{\mathrm{V}} = Me = \int_A \frac{\beta_x \, dA}{\dot{m}_{\mathrm{W}}} \tag{4}$$

The manufacturers of the cooling tower fills provide the information on the dependency of the Merkel number on the ratio λ of the dry air mass flow and the cooling water flow in their characteristic curves for the product:

$$Me = Me_{(\lambda=1)} \cdot \lambda^m \tag{5}$$

In Anglo-Saxon countries, the following nomenclature is often used for the description of the fill characteristics curves:

$$\frac{KaV}{L} = f(L/G) = f(1/\lambda) \tag{6}$$

Therefore, it is the responsibility of the manufacturer to provide the designer with precise fill characteristics for the thermal performance of the fills based on high-quality measurements within special testing facilities by application of relevant test conditions for real operation.

The convective heat transfer coefficient is calculated based on the Lewis-analogy taking into account a correction for one-directional diffusion at the phase interface [6]:

$$\frac{\alpha}{\beta_x} = c_{pm} \cdot Le^{(1-n)} \cdot \frac{\left(p''_{S,W} - p_{S,A}\right)}{\left(p - p''_{S,W}\right) \cdot \ln\left(p - p_{S,A} / p - p''_{S,W}\right)} \tag{7}$$

Here, c_{pm} is the specific heat capacity of wet air related to the dry air mass:

$$c_{pm} = c_{p,A} + c_{p,S} \cdot X_A \tag{8}$$

The Lewis number and the exponent n depend on the flow type and are based on experimental investigations. The determination of the values for the investigated cooling tower is reported in Section 3.2.1.

For cooling tower performance calculations with conventional schemes, it is of great importance to calculate precisely the demand curve of the cooling tower, which depends on the specific design data of the cooling tower. The point of intersection of the demand curve and the cooling fill characteristic curve gives as a result the design value for the ratio λ as shown in Fig. 4. As the precise calculation of the cooling tower demand curve is a very difficult task because of the great number of influence parameters and the complex interaction of the cooling tower aerodynamics and thermodynamics, there is a great uncertainty within this approach.

The great advantage of the presented comprehensive numerical approach is that in a converged solution, the calculated operating point will automatically fulfil the necessary requirements. The inlet air mass flow is the result of the numerical simulation and it depends on the iterated heat transfer (based on the correlations), the pressure drop (based on further correlations), the cooling tower geometry, ambient conditions and inlet water flow conditions. The numerical results provide not only the integral values for transferred heat and the cold water temperature, but also the local data for the flow field, local heat and mass transfer values and local cooling down of the cooling water film. When the numerical model has been validated for a specific cooling

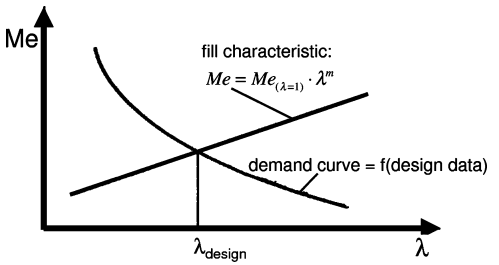

Figure 4: Conventional design approach based on characteristic curve and separated calculation of the cooling tower demand curve.

tower, parametric studies on the variation of the ambient conditions (e.g. ambient temperature, pressure and humidity) from the design values allow a precise determination of the effects for the cooling tower performance, e.g. the calculated cold water temperature. This includes cross wind situations or installation of different fill types or change of the fill arrangements. Another topic of interest might be an inhomogeneous distribution of the sprayed water instead of a homogeneous distribution. Thus, designers and operators of cooling towers get an improved decision basis for new cooling tower arrangements or retrofit measures for existing cooling towers.

3 Validation

3.1 Aerodynamic code validation

Based on experimental results [7, 8] for the aerodynamics of a cooling tower model, the validation of the basic CFD code has been performed. The original cooling tower has a total height of H_{tot} = 120 m, a waist height (smallest diameter) of $H_w = 0.79H_{tot}$, and a base diameter of D_b = 100 m. In the experiments, the geometry model of the cooling tower has a scaling factor of 1:275. For aerodynamic investigations of a group arrangement, further experiments include an additional cooling tower model that has been placed at a distance of $d = 1.87D_b$ behind the first model. The contour of the cooling towers has been modelled by a circular arc that can be derived from the given geometric parameters.

The three-dimensional grid consists not only of the cooling tower; it is also necessary to model the environment of the cooling tower with boundaries far away from the cooling tower such that undisturbed pressure distributions can be prescribed, which, under these conditions, have only a negligible influence on the calculated pressure distributions of the cooling tower. Here, all boundaries of the three-dimensional grid in all three coordinate directions have been placed at least at a distance of three times the base diameter away from the cooling towers. Figure 5 shows a close-up of the numerical grid of the cooling tower. The grid for the external flow part consists of approximately 550,000 finite volume cells. The internal flow region of the cooling tower that consists also of the air supply channel and a diffuser has been modelled with approximately 600,000 additional cells. Furthermore, the pressure losses of two sieves, one placed at the diffuser outlet and

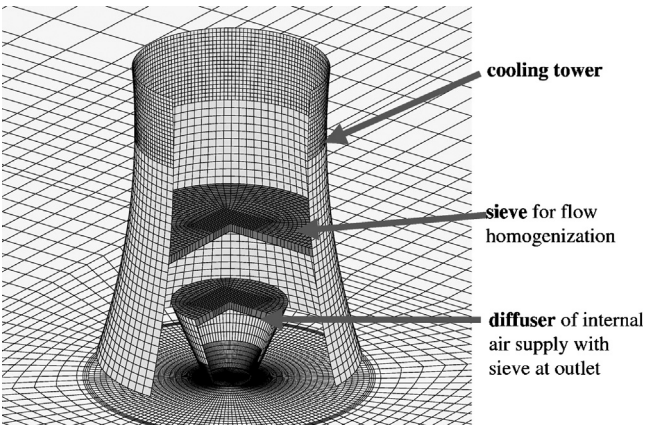

Figure 5: Numerical model and grid of single cooling tower.

the other one placed in front of the tower waist have been taken into account by a pressure loss model based on pressure loss coefficients.

A fully turbulent flow has been reached in the experiments by additional turbulators on the surface of the cooling tower. Thus, the standard-k, ε-model with an additional wall roughness parameter has been used in the numerical simulations. Furthermore, calculations with the original geometry size have been performed. In that case, the flow has a very high Re number and a turbulent boundary layer is established. Therefore, the calculations can be performed with a hydraulic even surface, means without an additional roughness parameter.

For the cross wind simulation, a velocity profile has to be prescribed at the inlet boundary, which should be an approximation of the atmospheric boundary layer. This is reached by a velocity distribution in dependency of the atmospheric height z in the following exponential law [8]:

$$\frac{c(z)}{c_\infty} = \left(\frac{z}{z_\infty} \right)^{0.25} \tag{9}$$

In the investigated cases of a single cooling tower and a group arrangement of two cooling towers, the undisturbed velocity c_∞ at the height of the cooling tower exit has been $c_\infty = 2.2$ m/s.

3.1.1 Results for single cooling tower

Based on the measured pressure distribution (timely averaged values) on the cooling tower surface at the waist height of $0.79H_{\text{tot}}$, a comparison of the pressure coefficients

$$c_p = \frac{p - p_\infty}{(1/2) \cdot \rho \cdot c_\infty^2} \tag{10}$$

with the calculated values can be given in Fig. 6.

The values are displayed in polar coordinates. The 0°-position is the stagnation point of the cooling tower. Measured values are available for the hydraulic even and hydraulic rough surfaces. It can be shown that the calculated pressure distribution is in good agreement with the measured values in both cases.

3.1.2 Results for cooling tower arrangement

The numerical grid is shown in Fig. 7. The arrangement of the cooling towers has been exposed to a cross wind with an offset angle of 15° to the centre connection line of the cooling towers. Thus, an asymmetric velocity and pressure distribution can be expected. This can be seen in the calculated pressure fields in Fig. 8a and b. Whereas Fig. 8a shows the experimental case with a rough

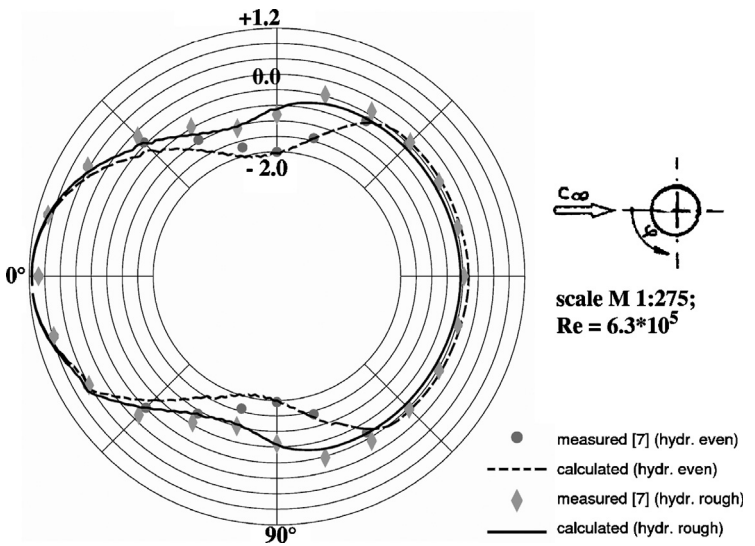

Figure 6: Distribution of c_p-values on the cooling tower surface (single tower) at a height of $0.79H_{tot}$.

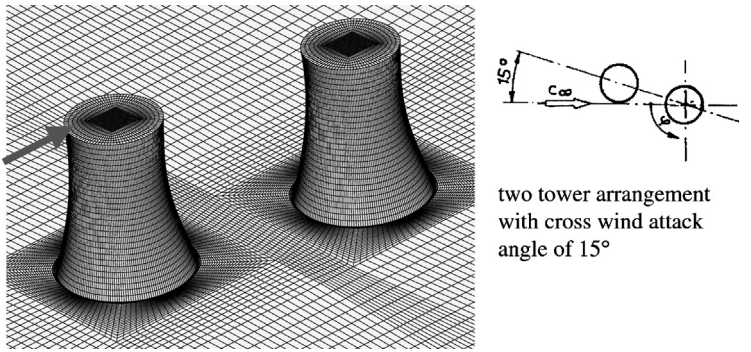

Figure 7: Numerical model and grid of two-tower arrangement.

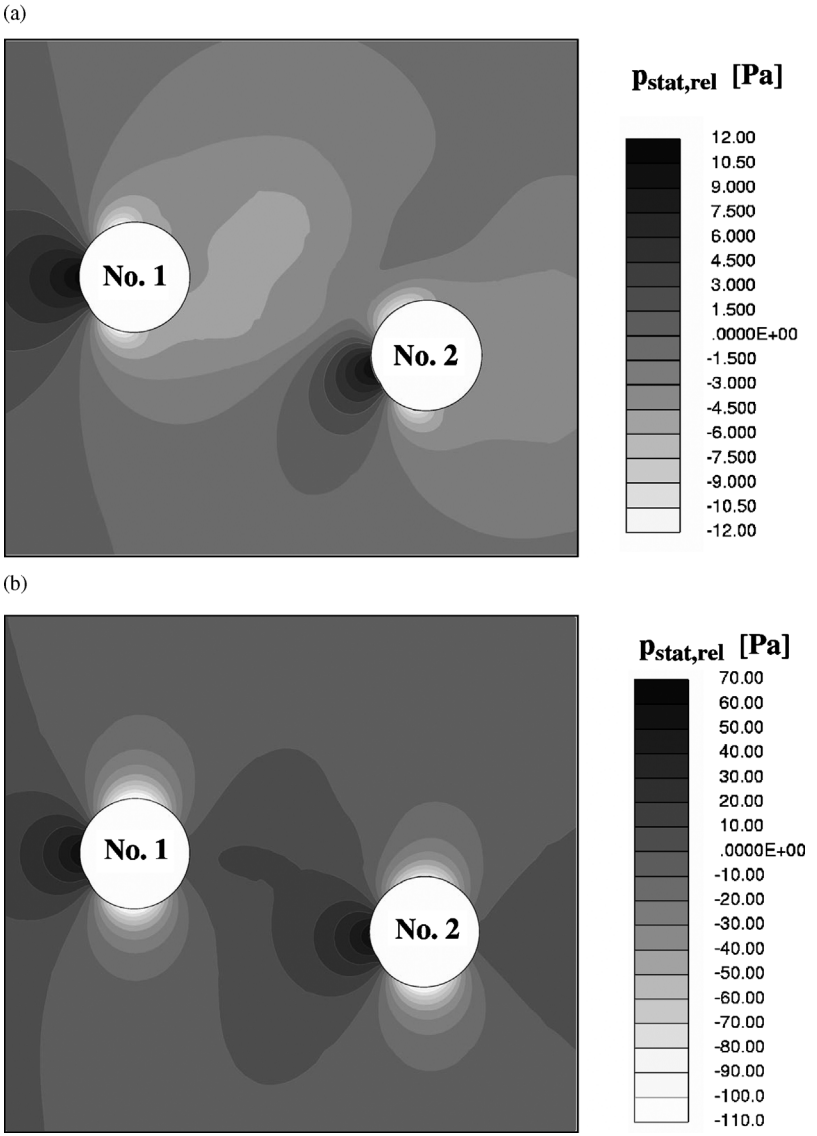

Figure 8: Calculated static pressure fields of the group arrangement at a height of $0.79H_{tot}$: (a) hydraulic rough surface, scale M 1:275, Re = 6.3×10^5; (b) hydraulic even surface, scale M 1:1, Re = 4.327×10^7.

surface, Fig. 8b shows the pressure field by taking into account the original cooling tower size and a hydraulic even surface. From the significant differences in the pressure field, it can be concluded that the experimental results cannot be transferred to the real flow situation. Due to the limitation of the

established Re number, aerodynamic interaction phenomena are overestimated in the experimental case.

With respect to the aerodynamic validation purpose, the comparison of the measured and calculated pressure coefficients for the second cooling tower in Fig. 9 shows a good agreement. It can also be seen that for the realistic very high Re number situation, there are significant differences in the distributions that are showing the reduced effect of the front cooling tower on the second one.

3.2 Validation of the coupled aerothermodynamic and heat transfer model

As the major purpose of the numerical investigation has been to get detailed results on the interaction of the cooling tower aerodynamics, thermodynamics and heat transfer, the basic models as described in Section 2 have been implemented to the code. Thus, it has been necessary to validate the code and models by comparison of the calculated data with results of a counterflow cooling tower that have been available from the operator of a power plant. Initial calculations for the validation purpose are without cross wind effects.

3.2.1 Numerical model and boundary conditions

Basic geometry parameters of the investigated cooling tower are a total height of H_{tot} = 117 m, a waist diameter of D_w = 61.3 m at a height of H_w = 90.7 m. Base diameter of the cooling tower is D_b = 92.8 m. A three-dimensional half-grid with symmetry condition has been generated for the cooling tower (Fig. 10). The half-grid contains approximately 500,000 cells. In the internal part of the cooling tower,

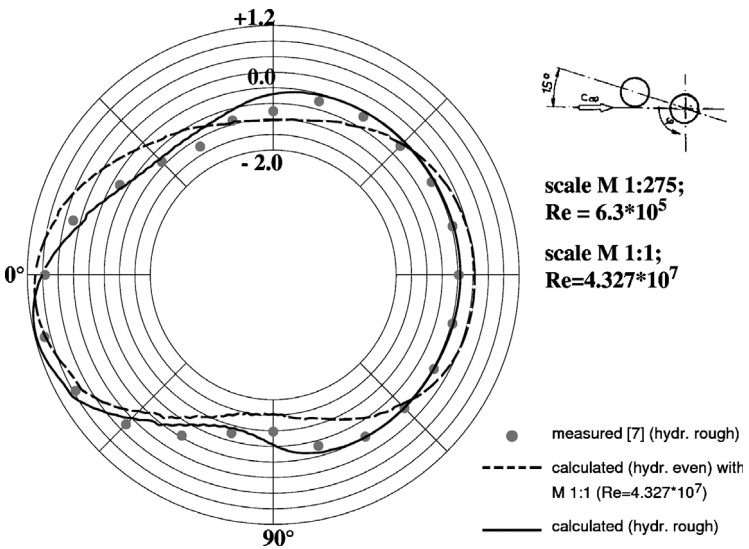

Figure 9: Distribution of c_p-values on the second cooling tower surface (group arrangement) at a height of $0.79H_{tot}$.

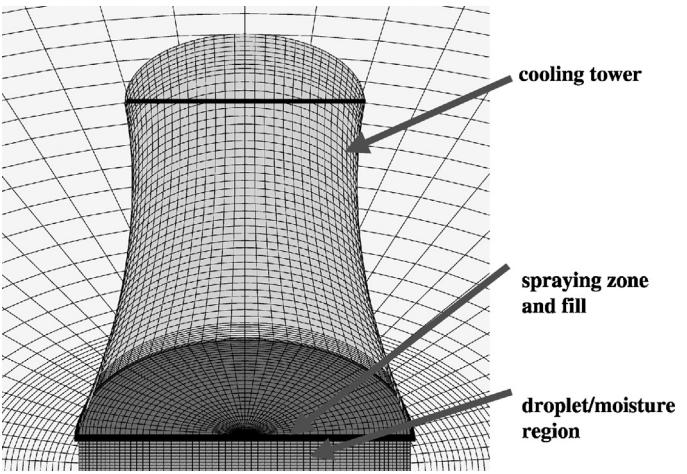

Figure 10: Numerical grid for coupled aerothermodynamic and heat transfer calculation (3D view into the tower).

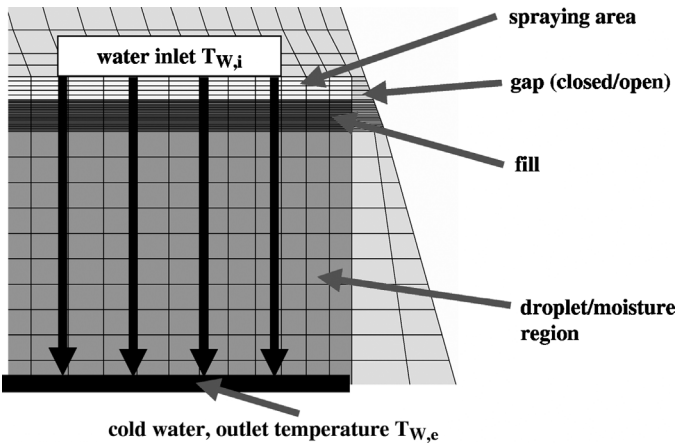

Figure 11: Detailed model description of the internal part of the cooling tower.

high-grid density modelling of the spraying zone, the fill volume, and the droplet/moisture region has been used as it can be seen in the zoomed area of Fig. 11.

The correlations of the evaporation number k_V (Me number) are needed for the heat transfer and mass transfer calculation in the spraying zone, fill volume and droplet/moisture region. Here, the necessary input has been provided by manufactures of the fill and by the power plant operators. In the investigated case conditions, the fill type of the cooling tower is fibrated concrete that has been replaced by a

plastic fill type (see Section 4.1). For the fill type, the following correlation in dependency of the local mass flow ratio λ can be given:

$$k_{V,fill} = 1.22 \cdot \lambda^{0.67} \tag{11}$$

For the spraying zone and droplet/moisture area, the following correlations have been used:

$$k_{V,spray} = 0.15 \cdot \lambda^{0.67} \tag{12}$$

$$k_{V,drop} = 0.03 \cdot \lambda^{0.67} \tag{13}$$

Based on the work provided by Poppe [6] the value of the Le number is Le = 0.865 and the exponent n in the Lewis analogy has a value of n = 0.33. Whereas an exponent of n = 1.0 is valid for a fully turbulent flow, a value of n = 0.33 indicates a flow with beginning thermal and hydrodynamic boundary layer formation. For the Lewis number, a value of Le = 0.865 is valid in a wide temperature range.

Furthermore, the pressure loss coefficients for the different regions have to be provided. These values have been provided by the designers of the cooling tower and the manufactures of the fill elements. Thus, these values depend on the specific design of the cooling tower. As precise values are part of the companies' proprietary, it is necessary to contact the manufactures so that such values can be provided. Here, the pressure loss coefficient for the fill elements itself is also dependent on the local flow velocity of the humid air. For velocities from v = 1 m/s to v = 2.5 m/s the loss coefficient is decreasing from ζ = 18 to ζ = 10.8. For the moisture/droplet region loss coefficients from ζ = 21.1 for v = 1 m/s to ζ = 12.6 for v = 2.5 m/s can be provided. For the spraying zone the values for the loss coefficients are ζ = 7.03 for v = 1 m/s to ζ = 4.2 for v = 2.5 m/s.

Finally, some basic thermodynamic data for the cooling tower operation are needed as input data (boundary conditions). These values are the air pressure (p_0 = 1013.0 hPa), the air temperature (T_A = 282.65 K), humidity (φ = 77.17%), water inlet temperature ($T_{W,i}$ = 307.35 K), and the water mass flow ($m_{W,i}$ = 58500.0 t/h). Due to the huge size of the cooling tower, the atmospheric layering of pressure and temperature as a function of the height has to be taken into account at the far field boundaries of the grid.

The dry air mass flow ($m_{A,dry}$) and the cold water temperature ($T_{W,e}$) are results of the numerical simulation. Thus, the local mass flow ratio Λ distribution will be also a calculation result at the end of the numerical iteration process. Of course, the local velocity field, local heat fluxes, and local mass fluxes are also a result of the CFD analysis. Thus, the great advantage of this comprehensive CFD approach is not only the precise calculation of the integral result values of the cooling tower but also the inclusion of several influences on these values for a systematic investigation on the improvement potential.

3.2.2 Aerothermodynamic calculation results

The calculated cold water temperature is the most critical parameter with respect to the calculated performance of the cooling tower. Initially, the temperature values for the water-side of the simulation have been set equally to $T_{W,i}$ = 307.35 K, that is the inlet warm water temperature. During the iteration process, the calculated cold water temperature decreases with ongoing calculation with only few numerical instability. This has been documented by the graph in Fig. 12, which shows the calculated cold water temperature during the iteration process. Finally, a converged value of $T_{W,e}$ = 295 K has been reached after 1500 steps with only minor further change. The final calculation value $T_{W,e}$ = 294.96 K is very close to the target design value of 294.75 K and clearly within a confidence level of ±0.5 K requested by the cooling tower designers.

Table 1 lists the most important integral values of the numerical simulation. The comparison of the total transferred heat shows that there is only a 1.8% difference

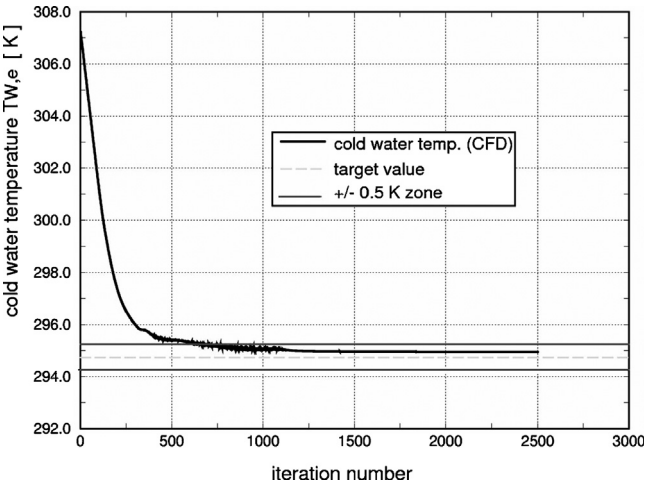

Figure 12: Cold water temperature calculation.

Table 1: Integral results on transferred heat and mass flow.

	Calculation		Design point
Cold water temperature	294.960 K		294.750 K
Total heat (transferred from water)	835.87 MW		850.0 MW
Convective heat	226.74 MW	27.13%	
Evaporation heat	609.13 MW	72.87%	
Total transferred heat in spraying area	76.75 MW	9.18%	
Total transferred heat in fill region	577.51 MW	69.09%	
Total transferred heat in droplet region	181.61 MW	21.73%	
Evaporated water mass flow	246.98 kg/s	1.52%	
Dry air mass flow	13779 kg/s		13390 kg/s
Averaged cooling tower outlet temperature	298.93 K		

between the value obtained from calculation and the cooling tower design value of 850 MW. The dry air mass flow is only 2.9% higher than the design value, which is also an acceptable deviation as the dry air mass flow is a calculated value based on the full aerothermodynamics and not a boundary condition.

Based on the local values in the flow field, one can distinguish precisely between the transferred convective heat and the evaporation heat, which is the major part (72.87%) of the heat transferred from the water side. Furthermore, it can be distinguished between the heat transferred in the spraying area, the fill, and the moisture/droplet region (Table 1). The evaporated water mass flow is 246.98 kg/s (1.52% of inlet water mass flow).

The flow visualization by flow vectors in a two-dimensional sectional cut is presented in Fig. 13. The dry air is sucked into the tower at the bottom and then turned into vertical direction so that only a minor part of the air streams through the complete droplet/moisture region until the centre of the tower. Then, the flow direction is homogenized in the fill area by the fill installation. Maximum flow velocities in the centre region of the tower are approximately 8 m/s. Furthermore, it can be seen in the zoomed region (Fig. 13b) that for the stationary case and without side wind effects no cold air entry in the tower exit area close to the tower rim can be observed.

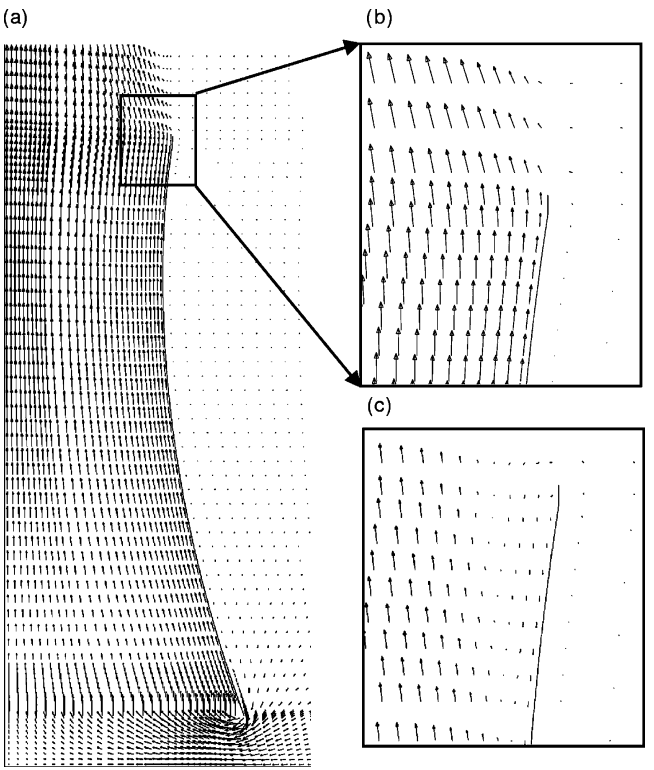

Figure 13: Cooling tower flow field: (a) flow vectors; (b) detail of outlet flow (closed gap); (c) detail of outlet flow (open gap).

The situation is different in the case, if the circular gap, as indicated in Fig. 11, is opened in the calculation model. In that case (Fig. 13c), a part of the inlet air is able to flow through the gap and leads to a low kinetic boundary layer flow. As a result, some part of the environmental cold air is able to generate a partly blockage of the tower outlet area close to the tower rim. A recirculating area of cold air can be observed. Overall performance of the cooling tower is significantly reduced. The simulation underlines the importance of the typical design feature to close gaps in the fill area near to the cooling tower wall.

4 Influences on the cooling tower performance

Based on the validation calculation of the cooling tower as shown in Section 3.2, the influence of several design features on the cooling tower performance is investigated by application of the numerical method.

4.1 Different fill types

With respect to the calculations for validation (reference case), the fill type has been fibrated concrete. It has been replaced by a modern plastic fill type as shown in Fig. 14 for an example. Such modern fill types are characterized by an improved heat transfer, low pressure losses and a high life-span.

The correlations of the evaporation number k_V are needed for the new fill type. The following correlation in dependency of the local mass flow ratio λ can be given:

$$k_{V,\text{fill}} = 1.92 \cdot \lambda^{0.633} \tag{14}$$

For the spraying zone and droplet/moisture area, the following correlations have been used:

$$k_{V,\text{spray}} = 0.15 \cdot \lambda^{0.633} \tag{15}$$

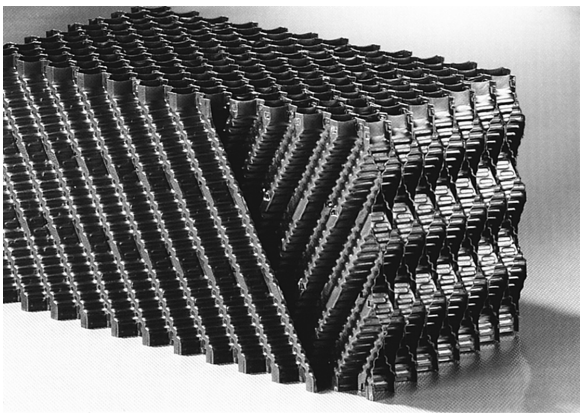

Figure 14: Typical plastic fill element for cooling tower application.

$$k_{V,drop} = 0.03 \cdot \lambda^{0.633} \tag{16}$$

Furthermore, the pressure loss coefficients for the different regions have to be provided. The pressure loss coefficient for the fill elements itself is dependent on the local flow velocity of the humid air. For velocities from $v = 1$ m/s to $v = 2.5$ m/s the loss coefficient is decreasing from $\zeta = 19.25$ to $\zeta = 11.52$. For the moisture/droplet region loss coefficients and the spraying zone, the same pressure loss coefficients have been applied as for the reference calculation (see Section 3.2.1).

Whereas the environmental conditions in the calculation are the same as in the reference case, some operating parameters have been changed (Table 2). The water inlet temperature is $T_{W,i} = 306.05$ K, and the inlet water mass flow $m_W = 63{,}000.0$ t/h (17500 kg/s). Initially, the temperature values for the water-side of the simulation have been set equally to $T_{W,i} = 306.05$ K, that is the inlet warm water temperature. During the iteration process, the calculated cold water temperature decreases with ongoing calculation and shows again an excellent convergence behaviour. That has been documented by the graph in Fig. 15. Finally, a converged value of

Table 2: Comparison of the operating conditions.

	Plastic fill type	Fibrated concrete fill type
Environmental temperature	282.65 K	282.65 K
Humidity	77.17%	77.17%
Environmental air pressure	1.013 bar	1.013 bar
Water inlet temperature	306.05 K	307.35 K
Inlet water mass flow	17500 kg/s	16250 kg/s

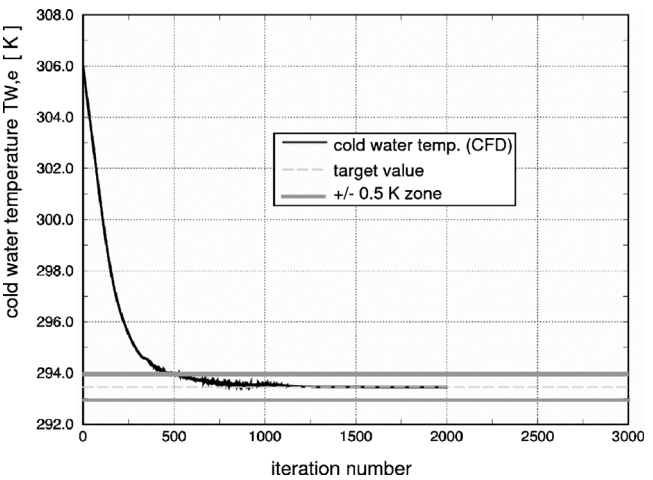

Figure 15: Cold water temperature calculation.

Table 3: Integral results on transferred heat and mass flow.

	Calculation		Design point
Cold water temperature	293.455 K		293.450 K
Total heat (transferred from water)	914.35 MW		915.0 MW
Convective heat	252.63 MW	27.63%	
Evaporation heat	661.72 MW	72.37%	
Total transferred heat in spraying area	55.60 MW	6.08%	
Total transferred heat in fill region	699.51 MW	76.50%	
Total transferred heat in droplet region	159.24 MW	17.42%	
Evaporated water mass flow	267.90 kg/s	1.53%	
Dry air mass flow	14137 kg/s		13230 kg/s
Averaged cooling tower outlet temperature	300.28 K		

$T_{W,e}$ = 293.455 K has been reached. That is almost identical to the design value (Table 3) and, therefore, clearly within a confidence level of ±0.5 K requested by the cooling tower designers.

Table 3 also lists the most important integral values of the numerical simulation. The comparison of the total transferred heat shows that this value is also almost identical to the design value of 915 MW. Compared to the reference case this means a significant increase in total heat transferred within the cooling tower (+7.6%). Thus, this improvement has a significant effect on the thermal efficiency of the steam cycle in the power plant. However, the percentage distribution of the heat transferred in the different regions of the cooling tower has only minor changes. The calculated dry air mass flow is approximately 6.8% higher than the design value.

One of the great advantages of the CFD approach is that detailed information on the local flow field is available. As an example, Fig. 16 shows the velocity distributions along section lines at different heights in the cooling tower. Thus, it can be shown that different velocity distributions are predicted for the different fill types. This is especially the case for the outlet distribution. For the simulation with plastic fill type, the bulk velocity is reduced, whereas the higher velocities close to the tower walls will lead to an increased kinetic energy in the boundary layer flow. That is of advantage with respect to the danger of local recirculation in the region of the cooling tower rim.

4.2 Geometry of the cooling tower rim

Further numerical simulations with the plastic fill type focus on another detail of the construction of the cooling tower that is the structure of the cooling tower rim. In the previous simulations, the cooling tower rim has been modelled in a simple way, but with respect to the statics of the cooling tower, it is necessary to add a special rim structure. Such structures stabilize the cooling tower and can be located at the outer or inner side of the cooling tower rim. Figure 17 shows a stabilizing structure at the inner rim side.

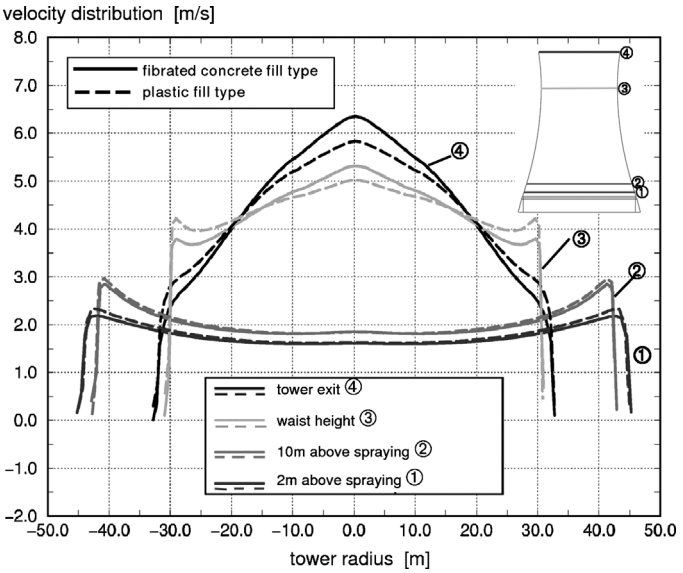

Figure 16: Velocity distribution in the cooling tower for different fill types.

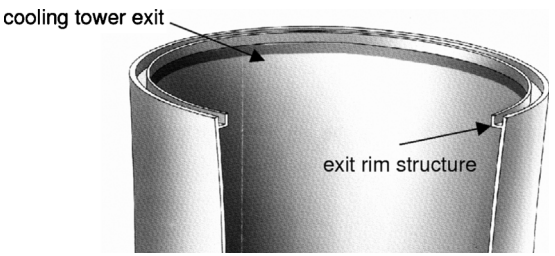

Figure 17: Stabilizing structure at the inner rim side.

Due to the fact, that the inner rim structure reduces the open exit surface of the cooling tower, an increase in the calculated cold water temperature of 0.175 K ($T_{W,e}$ = 293.63) is predicted, that is still by far within the confidence level of ±0.5 K requested by the cooling tower designers. The calculated dry air mass flow is reduced to 13830 kg/s compared to the 14137 kg/s for the calculation without the inner rim structure. Thus, the calculated air mass flow is now 4.5% higher than the design value. Based on these results, it might be of advantage to install a rim structure at the outer side. This might be correct with respect to the viewpoint of the aerothermodynamics without flow instabilities at the cooling tower exit, but a simulation under the same conditions but with opened gap between the fill and the tower wall disclose the great advantage of the inner rim structure for stabilizing the tower exit flow. Whereas in the case without the inner rim structure an unstable flow with local recirculation near the cooling tower rim can be observed in Fig. 18a, the situation is significantly improved for the case with inner rim structure

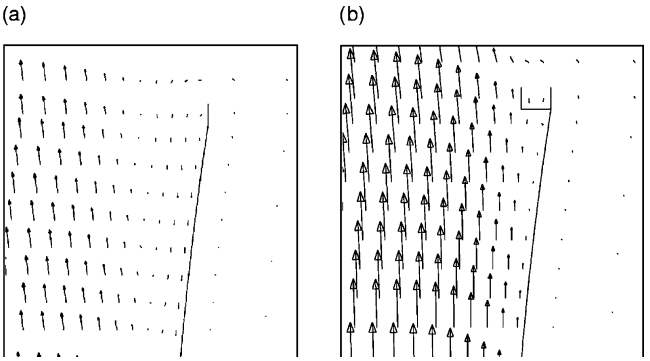

Figure 18: Flow vector at tower exit (tower rim): open gap (a) without and (b) with inner rim structure.

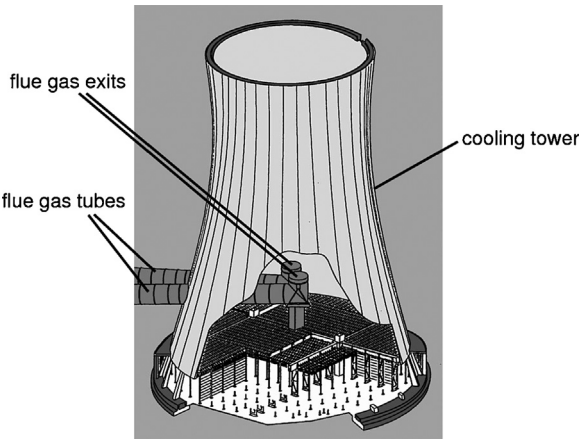

Figure 19: Natural draft cooling tower with additional flue gas operation.

(Fig. 18b). In that case, the velocity vectors show not only increased velocities at the exit but also that the recirculating flow area has vanished.

4.3 Additional flue gas discharge operation

Additional flue gas discharge operation for cooling towers has been established in recent years. In that case, the additional construction of a high chimney for the flue gas is not necessary. Thus, the costs for the construction of the power plant are reduced. Another advantage might be seen in the optical appearance of the power plant. Figure 19 shows a drawing for a typical construction of a cooling tower with additional flue gas discharge operation.

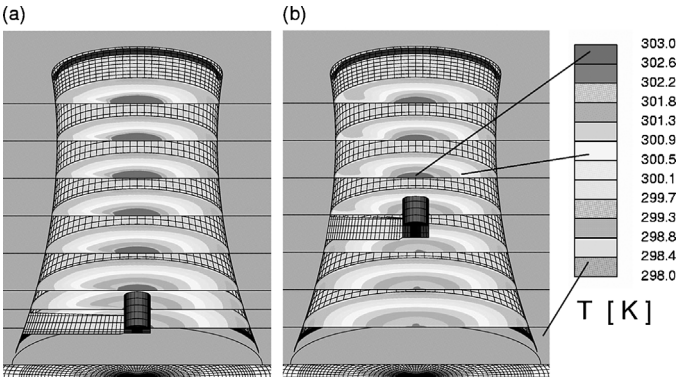

Figure 20: Temperature distributions for the cooling tower (plastic fill type, inner rim structure, closed gap) with additional flue gas operation: flue gas outlet at (a) H_{flue} = 13 m and (b) H_{flue} = 51 m.

However, several questions are of high interest in case an additional flue gas operation is implemented. At first, there is the question on the changed aerothermodynamics of the cooling tower. Furthermore, it is of significant importance to avoid any contact of the aggressive gases with the tower walls. Thus, numerical simulations with additional flue gas outlets in two different height, H_{flue} = 13 m and H_{flue} = 51 m, have been performed. The calculations have been executed with plastic fill type, inner rim structure and a closed gap between the fill and the tower wall.

Figure 20a and b show the three-dimensional temperature distribution in cutting planes at different tower heights for both cases. The high temperatures are in the centre region of the cooling tower. There is no hint that in case of stable operation of the cooling tower there is a danger of flue gas contact with the tower walls. Furthermore, the integral evaluation of the results shows that there is only a minor effect of the additional flue gas discharge operation on the aerothermodynamics of the cooling tower. For a height of H_{flue} = 13 m, there is a very slight improvement of the cold water temperature with a reduction of just –0.004 K. Some small blockage effects of the flue gas piping are compensated by a small improvement of the draught in the tower due to the warmer flue gases. In the case of an additional flue gas discharge operation with an outlet height of H_{flue} = 51 m, there is a very slight increase in the cold water temperature due to the blockage effect and only very minor improvement of the draught in the tower. However, to reduce the danger of a flue gas contact with tower walls, it might be even more secure to install the flue gas outlet at a high position as all negative effects on the aerothermodynamic performance of the cooling tower can be stated as negligible.

5 Cross wind effects on the cooling tower performance

A final set of numerical simulations for the cooling tower application deals with the impact of different cross wind situation, i.e. different wind velocities. It is

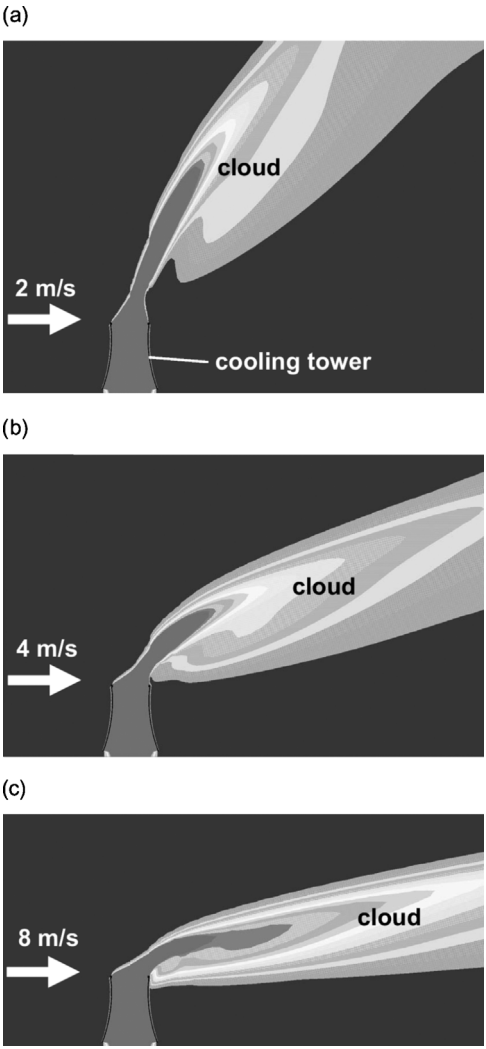

Figure 21: Temperature distributions for visualization of the cooling tower cloud propagation under cross wind effects: cross wind velocity of (a) 2 m/s, (b) 4 m/s and (c) 8 m/s.

well known that the interaction of the cooling tower flow and the cross wind can lead to a situation with a large region of cold air entering the tower exit. This phenomenon leads to a reduction in the effective cooling tower outlet area and, thus, has also a significant negative impact on the cooling tower performance and, furthermore, on the steam cycle performance. Thus, such operating situations have to be avoided or at least to be reduced in size by a modern design of the cooling tower.

5.1 Stable configurations

The modelling of the cross wind is done in the same way as described in the Section 3.1 for the aerodynamic validation. The cooling tower model that has been used contains the plastic fill type, the inner rim structure and a closed gap between the fill and the tower wall. Calculations (three-dimensional) have been performed with different wind velocities of $v_w = 2$ m/s, $v_w = 4$ m/s, $v_w = 8$ m/s, and $v_w = 14$ m/s.

Figure 21a–c shows the propagation of the cooling tower cloud due to the impact of different wind velocities. For all velocities, a stationary solution has been reached as shown in Fig. 21a–c. Therefore, the numerical simulations do not show any hint for a cold air ingestion at the tower exit. Nevertheless, an impact on the cooling tower performance, i.e. the cold water temperature, can be found as described by Fig. 22. For very small cross wind velocities of approximately $v_w = 2$ m/s a slight improvement, i.e. a reduction of the cold water temperature can be observed. With further increasing cross wind velocities, there is a significant negative effect on the cooling tower performance and the cold water temperature increases. As it is shown by the curve in the diagram of Fig. 22, the increase in the cold water temperature is not linear but follows a parabolic shape and the situation worsens for high cross wind velocities. However, cold air ingestion is even not observed for the highest investigated cross wind velocity of $v_w = 14$ m/s.

The reasons for the stable behaviour of the cooling tower can be found in the advantageous tower design. As it has been shown in Section 4.2, the inner rim structure has a stabilizing effect on the flow regime near to the tower rim. Furthermore, the plastic fill type leads to a boundary layer flow with a higher kinetic energy (see Section 4.1). Altogether, these two design features lead to a stable flow situation at the tower outlet even in a cross wind situation of up to $v_w = 14$ m/s.

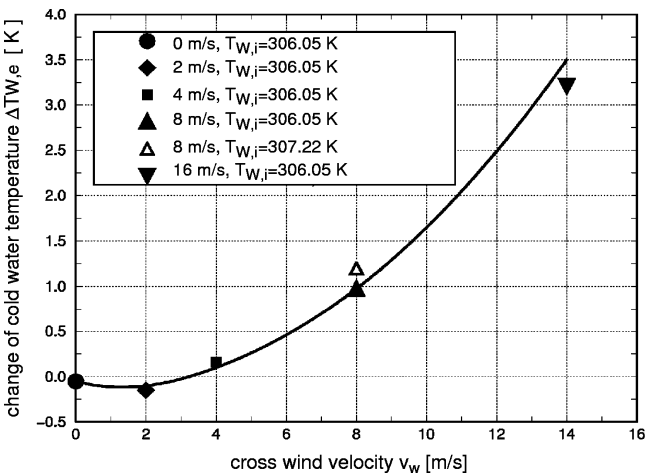

Figure 22: Calculated change of cold water temperatures for different cross wind velocities.

5.2 Unstable configuration with cold air ingestion

Based on the understanding of the positive effects of the inner rim structure and the plastic fill type on the exit flow of the cooling tower, a more unstable situation has been expected for a cooling tower simulation without the inner rim structure and the fibrated concrete fill type. Furthermore, the gap between the fill and the tower wall has been opened in the numerical model as investigations presented in Section 3.2.2 have shown that an open gap leads to a recirculating flow area at the tower rim even in the case without cross wind. The three-dimensional simulation has been started based on the case without cross wind as the initial flow and temperature field and with a low cross wind velocity of v_w = 2 m/s. Figure. 23 shows the calculated cold water temperature during the iteration process. Whereas in other simulation a good convergence has been observed, the situation is now different. A convergence of the cold water temperature has not been reached. Instead, there is a periodic fluctuation of the cold water temperature with the time steps.

Figure 24 shows the visualization of the temperature field at four different time steps as indicated in Fig. 23. At position 1 (Fig. 24a), there is a low cold water temperature and there is only a minor area of cold air ingestion near to the tower rim. Then, with increased cold air ingestion as shown in Fig. 24b for position 2, the cold water temperature increases rapidly. It reaches its maximum at position 3. Figure 24c shows for that case that a major part of the tower outlet is blocked by cold air. However, warm air in the lower part of the tower has started to push the cold air towards the outlet. Figure 25 shows a three-dimensional view of the temperature distributions for position 2 and position 3. Thus, it becomes even more obvious how deep the cold air can penetrate into the interior of the cooling tower.

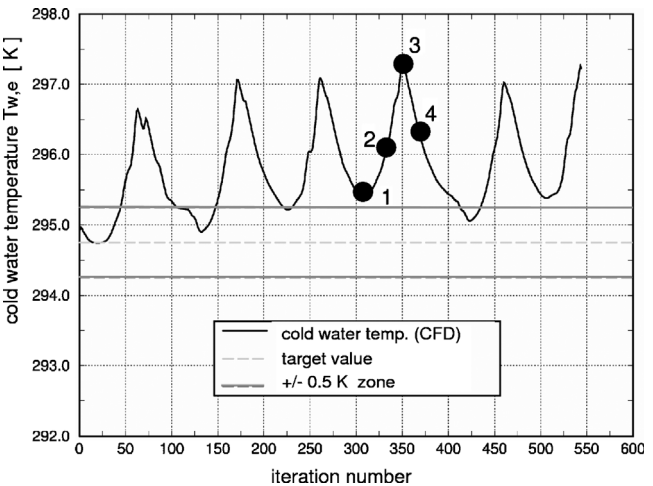

Figure 23: Cold water temperature calculation, cross wind velocity 2 m/s, cooling tower *without* inner rim structure.

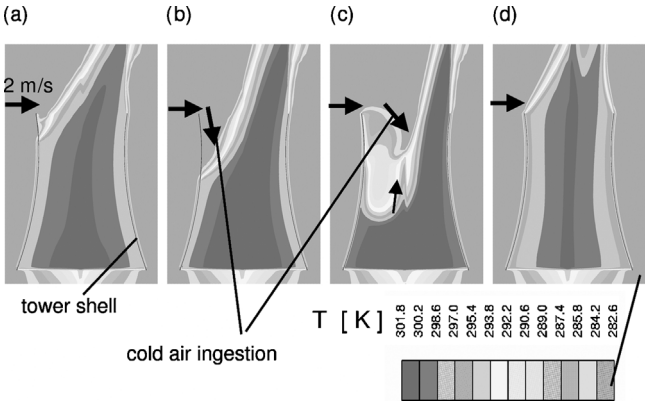

Figure 24: Temperature distribution at indicated iteration steps, cross wind velocity 2 m/s, cooling tower *without* inner rim structure: (a) position 1, (b) position 2, (c) position 3 and (d) position 4.

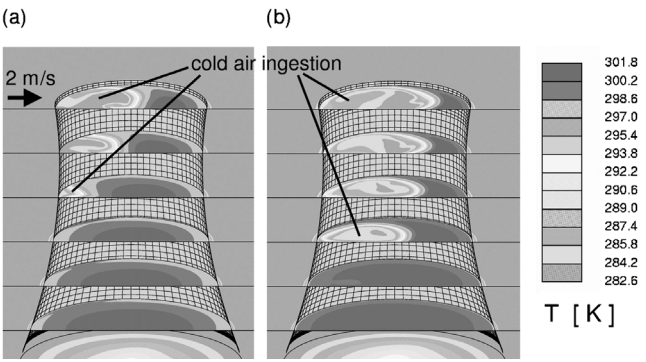

Figure 25: Temperature distribution (3D view) at indicated iteration steps, cross wind velocity 2 m/s, cooling tower *without* inner rim structure: (a) position 2 and (b) position 3.

At position 4 (Fig. 24d), the warm air fills the cooling tower completely but is still disturbed at the outlet. However, the curve for the cold water temperature in Fig. 23 shows that it has decreased now rapidly and will further decrease until a similar situation is reached as it has been at position 1. Then, the next cycle starts. Thus, the effect of cross wind for cooling tower design with significant deficiencies might lead to a timely periodic cold air ingestion as it has been shown by Figs. 23–25. However, it has to be taken into account that the results shown in Section 5.2 are only of limited numerical value as the calculation is not unsteady, but results are obtained of a periodic numeric instability in a steady calculation using a time-marching scheme. Unsteady calculations of the cold air ingestion phenomenon in case of a cross wind situation have not been performed now by the authors

due to the enormous calculation efforts. With increased performance of modern PC-Clusters, this possibility should soon be in reach for validation of the observed and described phenomenon.

Nomenclature

A (m^2)	area
D (m)	diameter
G (kg/s)	mass flow rate of dry air
H (m)	height
L (kg/s)	mass flow rate of water
Le (–)	Lewis number
$\dot{Q}$ (J/s)	heat flow rate
Ka (kg/(m^3 s))	mass transfer coefficient
Me (–)	Merkel number
Re (–)	Reynolds number
T (K)	temperature
V (m^3)	volume
X (–)	water content (X := mW/mA, dry)
c (m/s)	velocity
c_p (J/(kg K))	specific heat capacity
cp (-)	pressure coefficient
c_W (J/(kg K))	specific heat capacity of water
d (m)	distance
h (J/kg)	specific enthalpy
k_V (–)	evaporation number
m (kg)	mass
$\dot{m}$ (kg/s)	mass flow rate
p (N/m^2)	pressure
v (m/s)	velocity
z (m)	vertical coordinate

Greek letters

α (W/(m^2 K))	heat transfer coefficient
β_x (kg/(m^2 s))	mass transfer coefficient
λ (–)	ratio of dry air mass flow and cooling water
ρ (kg/m^3)	density
ζ (–)	pressure loss coefficient

Subscripts

A	air, air-side
S	steam, vapour
W	water, water-side

b	base
e	exit, outlet
ev	evaporation
drop	droplet/moisture region
dry	dry air
fill	cooling fill
flue	flue gas
i	inflow, inlet
rel	relative (with respect to reference value)
spray	spraying zone
stat	static
tot	total
w	waist
w	wind (velocity)
∞	infinity

Superscripts

″	condition at phase liquid/gas interface

References

[1] *Cooling Tower Performance Curves*, Cooling Tower Institute: Houston, TX, 1967.
[2] Kelly, N.W., *Kelly's Handbook of Crossflow Cooling Tower Performance*, Neil W. Kelly and Associates: Kansas City, MO, 1976.
[3] Majumdar, A.K., Singhal, A.K. & Spalding, D.B., Numerical modeling of wet cooling towers – Part 1: Mathematical and physical models. *Journal of Heat Transfer*, **105**, pp. 728–735, 1983.
[4] Majumdar, A.K., Singhal, A.K., Reilly, H.E. & Spalding, D.B., Numerical modeling of wet cooling towers – Part 2: Application to natural and mechanical draft towers. *Journal of Heat Transfer*, **105**, pp. 736–743, 1983.
[5] Star-CD Version 3.20, CD adapco Group, 2004.
[6] Poppe, M., *Wärme- und Stoffübertragung bei der Verdunstungskühlung im Gegen- und Kreuzstrom* (in German), PhD Thesis, Technical University of Hannover, 1972.
[7] Beger, G., Modellversuche zur Windlastbestimmung an Kühltürmen in Gruppenaufstellung (in German). *Energietechnik*, **42(2)**, pp. 45–48, 1992.
[8] Beger, G., Modelluntersuchungen der Strömungsverhältnisse im Kopfbereich von Naturzugkühltürmen (in German). *Energietechnik*, **40(4)**, pp. 135–139, 1990.